Chemical Engineering Science 186 (2018) 152–167

Contents lists available at ScienceDirect

Chemical Engineering Science

journal homepage: www.elsevier.com/locate/ces

Interrogating flow development and phase distribution in vertical and horizontal pipes using advanced instrumentation

M. Abdulkadir [a,*], V. Hernandez-Perez [b], C.A. Kwatia [c], B.J. Azzopardi [d]

[a] Department of Chemical Engineering, Federal University of Technology, PMB 65, Minna, Niger State, Nigeria
[b] Department of Mechanical Engineering, National University of Singapore, Singapore
[c] Petroleum Engineering Department, African University of Science and Technology (AUST), Abuja, Nigeria
[d] Process and Environmental Engineering Research Division, Faculty of Engineering, University of Nottingham, University Park, Nottingham NG7 2RD, United Kingdom

HIGHLIGHTS

- The vertical flow was seen to be fully developed whilst in rapid development for the horizontal flow.
- The phase distributions in vertical and horizontal flows are examined in detail.
- A plot of mixture velocity against void fraction may be used to provide an index of flow pattern.
- The determination of drift flux parameters for vertical and horizontal flows is carried out.

ARTICLE INFO

Article history:
Received 26 December 2017
Received in revised form 13 March 2018
Accepted 19 April 2018
Available online 21 April 2018

Keywords:
Void fraction
Drift-flux model
ECT
WMS
C_0
V_D
Flow patterns

ABSTRACT

The characterization of two-phase flow in both vertical and horizontal pipes is important in oil/gas transportation. As the pipe orientation may change from well to well, it is also important to understand the characteristic responses expected of a two-phase mixture to a change in pipe inclination. This study concerns the changes in the void fraction, structure frequency and structure velocity that occur within an air–silicone oil mixture as a function of the pipe orientation. Experimental data were obtained from the combined use of electrical capacitance tomography (ECT) and wire mesh sensors (WMS), which allow the 3D visualization of the flow patterns. The reported experiments were performed on a 67 mm diameter pipe, in a flow loop, in which a pipe section may be inclined at angles of between −5 or 90° to the horizontal. For this study, the inclined pipe was either set at an angle of 0 or 90 to the horizontal, which correspond to a horizontal or vertical pipe setting, respectively. The results of flow development using the PDF of void fraction obtained at 3 measurement locations; ECT 1, ECT 2 and WMS at 4.4, 4.489 and 4.92 m, respectively, showed that the flow is fully developed and statistically stable for the vertical two-phase flow. While on the other hand, the flow is in rapid development for the horizontal two-phase flow scenario at same liquid and gas superficial velocities. The processed data reveal the differences in flow distribution produced by the pipe inclination. Within the vertical pipe configuration spherical cap bubbles, slug and churn two phase flow patterns were observed, whilst plug, slug and stratified wavy two-phase flows were identified in the horizontal configuration of the pipe. It is concluded that a plot of mixture superficial velocity against average void fraction may be used to provide a qualitative assessment of the flow patterns observed, regardless of pipe inclination. The two-phase flow variables that are concluded to significantly influence the distribution coefficient, C_0, and drift velocity, V_D, are the pipe orientation and flow patterns.

1. Introduction

Multiphase flow research is a very important topic within the process industries. Most of the work in this field began by using air–water mixtures in either horizontal or vertical pipes Gomez et al. (2000). These studies provide fundamental knowledge with which to characterize the behaviour of multiphase flows in different pipe flow orientations. Many applications in industry may involve the transport of multiphase flow mixtures around pipe flow circuits that may contain several changes of level that may be connected by pipes of different orientations. However, to date

* Corresponding author.
E-mail address: mukhau@futminna.edu.ng (M. Abdulkadir).

https://doi.org/10.1016/j.ces.2018.04.039
0009-2509/

most of the published studies have been on either vertical or horizontal, without a detailed comparative analysis of the two-phase flow structures observed within both vertical and horizontal pipes.

1.1. Flow development

Brown et al. (1975) investigated experimentally the flow development leading to hydrodynamic equilibrium in annular flow in heated and unheated vertical 9.61 mm diameter pipes. They observed that the wave spectrum took fairly long distances to develop.

Wolf et al. (2001) experimentally investigated the flow development leading to hydrodynamic equilibrium in annular flow in heated and unheated vertical 31.8 mm diameter pipes. The mass flux of air and water that they considered are 10–120 kg/m^2 s and 71–154 kg/m^2 s, respectively. They reported that the parameters associated with the disturbance wave velocity and frequency (wave structure) showed only a small variation between dimensionless axial distances (L/D) of 100 and 300 for all the mass flux combinations of air and water.

Barbosa et al. (2001) and Wang et al. (2012) investigated flow development and wave behaviour in churn flow. However, their work was limited to the region near the entrance. Hazuku et al. (2008) measured experimentally the evolution of liquid film thickness and wave characteristics in a vertical 3 m long with 11 mm diameter pipe by means of a laser focus displacement technique. They concluded that the flow did not reach a developed state in the test section based on the fact that neither the liquid film thickness nor the wave frequency ceased to decrease as a function of distance.

Kaji et al. (2009) investigated experimentally the effect of flow development on the structure of slug flow in vertical pipes of internal diameters and lengths of 51.2 mm and 3.5 m and 52.3 mm and 9 m, respectively. They reported void fraction, frequencies of liquid slugs and Taylor bubbles and lengths of liquid slugs and Taylor bubbles at several distances from the inlet of the pipes. They concluded that the slug frequency showed a gradual decrease with distance which did not stabilize until the end of the test section. They also concluded that the lengths of the liquid slug and Taylor bubble increased with distance, reaching a somewhat stable value at L/D = 100.

Julia et al. (2009) investigated the axial flow development of flow patterns in vertical upward flow in an annulus. The inner and outer diameters of the annulus that they used are 19.1 and 38.1 mm, respectively, and a total vertical length of 4.37 m. However, they did only a few runs for churn and annular flows since they were not the main focus of their work.

Waltrich et al. (2013) investigated experimentally axial flow development of gas–liquid flow in a vertical 42 m long and 0.048 m internal diameter pipe. They compared different transitional models for slug, churn and annular flows against visual observations and the obtained results showed reasonable agreement at locations L/D = 560 and 820. They analyzed the behaviour of liquid holdup and frequency of flow structures (large waves, disturbance waves) for three locations at L/D = 102, 521 and 815 over a range of pressures between 1.4 and 5.2 bar. It was concluded that the liquid holdup showed significant axial variation at all monitored locations for higher liquid mass fluxes, while it appeared that a kind of developed flow was reached at L/D = 521 for lower liquid mass fluxes. The flow structure did not exhibit significant axial variation for dimensionless gas velocities (Wallis parameter) between 0.2 and 1.6.

Dinaryanto et al. (2017) carried out an experimental work on the initiation and flow development of an air–water slug flow in a 26 mm internal diameter horizontal pipe. They explained the slug initiation mechanism by visual observation and pressure fluctuation. The initiation of slug and slug frequency were obtained using two high video camera. They claimed that the liquid and gas superficial velocities played an important role in slug flow initiation and flow development. However, the discussion on flow development was subjective and they did not report at what L/D the flow was developed.

1.2. Phase distributions in vertical and horizontal pipes

The spatial distribution of the flow phases within a pipe significantly influence the accurate determination of both the pressure gradient and hydrodynamic characteristics. The primary characteristic of a multiphase flow system is the phase distribution, which is very complex to predict and resolve due to the existence of moving boundaries between different phases and the turbulent nature of the flow regime.

Shoham (2006) concludes that design methods require the satisfactory determination of the pressure drop, liquid holdup, and void fraction distributions of a transported fluid in order to optimally size flowlines and separation facilities for flow assurance purposes. Roitberg et al. (2007) recommends that investigations of two-phase pipe flows are very essential for various industrial applications that require reliable predictive quantitative solutions for design and maintenance. Thus, there is a need to predict and characterize flow regimes in greater detail.

Besides, many of the previous experimental void fraction distribution studies reported in the literature are restricted to the study of air/water system flows within small diameter pipes. Many process industry applications involve the flow of a mixture of fluids of varying physical properties, including oils of higher viscosity and surface tension that may significantly influence the phase distributions observed with a flow. Consequently, there is the need to experimentally determine, the void fraction distributions for low surface tension liquids other than water in vertical and horizontal pipes to provide reliable performance data that permits the economic design of production facilities.

In recent years, there have been several studies that have investigated two-phase flow behaviour in inclined pipes. Geraci et al. (2007) reports the results of an analysis of measurements of annular flow film thickness observed in a 38 mm pipe across a range of pipe inclinations. Hernandez-Perez (2008) reports data for gas–liquid flow in inclined pipes, mainly for slug flow, both of them using air–water mixtures. More recently, Hernandez-Perez et al. (2010), Szalinski et al. (2010) and Abdulkadir et al. (2014a) report the results of the two-phase flow characteristics for a range of gas–fluid mixtures they could identify from an analysis of data collected from advanced measurements recorded within a vertical pipe. The studies of Szalinski et al. (2010) and Abdulkadir et al. (2010) report the radial profiles of local void fractions observed within a vertical pipe. Abdulahi et al. (2011) summarizes the results of an analysis of the measurement data to determine the two-phase flow characteristics within a pipe inclined at 10° from both horizontal and vertical, whilst Abdulahi et al. (2011) describes an analysis of data recorded in an inclined pipe over a specified range of inclination angles, both of these studies employing an air–silicone oil mixture. Franca and Lahey (1992) report data for horizontal air–water two-phase flow having various flow regimes. Their analysis concludes that they could establish a correlation between experimental data and the drift-flux models. A review of the literature has been unable to reveal any recent studies that have reported a detailed comparison of the phase distributions observed for the flow of gas–liquid mixtures within vertical and horizontal pipes inclination with the behaviour predicted by suitable drift-flux models.

From the studies regarding flow development and detailed analysis of void fraction distributions, there emerges a clear need to

clarify flow development and analysis of void fraction in vertical and horizontal intermediate >55 mm diameter pipes transporting an air–silicone oil mixture. This work therefore aims to investigate experimentally flow development and detailed phase distributions in vertical and horizontal pipes using advanced instrumentation. Thus, this paper therefore provides insightful data and analysis for different two-phase flow parameters, such as void fraction, structure velocity and frequency. Based on this information, the effect of changing pipe inclination from vertical to horizontal on different aspects of gas–liquid flow in inclined pipes is investigated.

2. Experimental rig configuration

In order to carry out this research, two advanced flow measurement instruments were employed namely, the Wire Mesh Sensor (WMS), developed at Forschungszentrum Rossendorf–Dresden and electrical capacitance tomography (ECT) developed at Tomoflow–Process Tomography Limited. The WMS and ECT transducers were mounted in an inclinable two-phase flow facility at Nottingham. The outline detail of the experimental flow loop, is presented elsewhere, Hernandez-Perez et al. (2010), Azzopardi et al. (2010), Abdulkadir et al. (2011, 2013, 2014a, 2014b, 2015). All of the experiments described in this paper were carried out on an inclined closed ring pipe flow rig within the Engineering Laboratories of the Department of Chemical and Environmental Engineering at University of Nottingham. The experimental facility consists of a main test pipe section constructed from transparent acrylic glass. The 6 m test pipe section is of a 0.067 m internal diameter. The test pipe section is mounted on a rigid steel frame that may be rotated and allowed it to be fixed between −5° to 90° degree as shown in Fig. 1. The air is supplied from the laboratory main compressor, which maintains 6 Bar, however a pressure regulation valve is used to regulate the air supply to 2 Bar. The discharge is open to atmosphere, so the outlet pressure is near 0 Psig. At the inlet, the pressure varies depending on the flow conditions, due to the pressure drop. As a result, the pressure gage located after and next to the gas rotameters ranges from 0.5 to 8.9 Psig. The rest of the pressure drop occurs across the valve

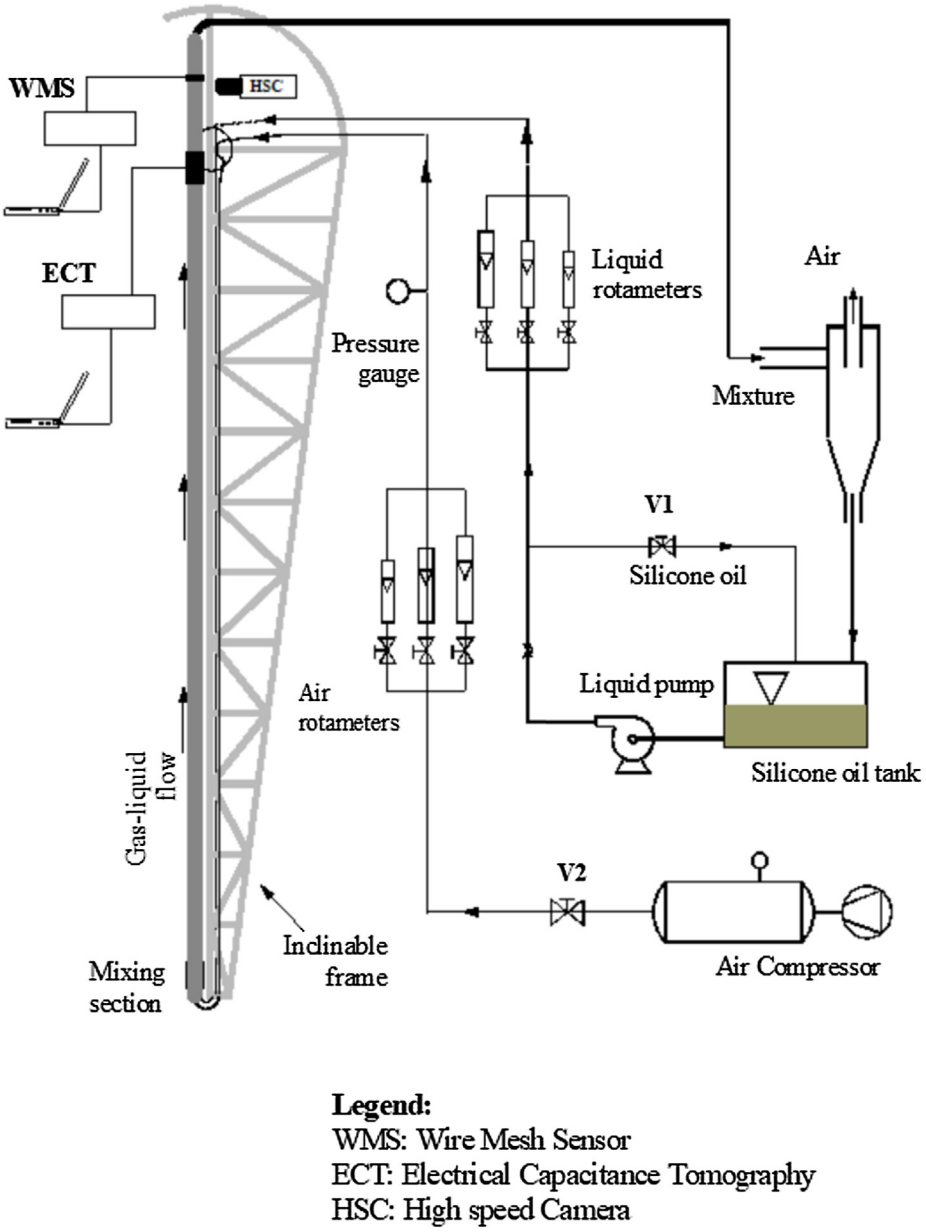

Fig. 1. Schematic diagram of the experimental facility employed in this work.

that controls the flow. The inlet section design ensures that the injected air is well mixed and equally distributed across the cross-section of the pipe. The flow rate through these valves was measured by the use of two parallel air flow rotameters as shown in Fig. 1. The range of the compressed air flow rates that may be delivered and measured by the two rotameters are in the ranges 10–1000 L/min. The compressibility of the gas phase was accounted for by expressing Q_G, and hence U_{SG}, as the volume or velocity corrected from the inlet pressure and temperature conditions to the pressure and temperature at section under consideration.

The rig is initially charged with an air–silicone oil mixture to study the flow regimes created by the circulation of various air–oil mixtures created by the controlled pumped circulation of the oil from the reservoir and the compressed injection of air at the base of the inclined riser pipe. The experiments were all performed at an ambient laboratory temperature of 20±0.5 °C and a pressure of 1 bar (a). The resultant flow patterns created for the range of air–silicone oil injection circulation flow rates studied were recorded using electrical capacitance tomography (ECT) and wire mesh sensor (WMS).

The sensors are described in detail in Prasser et al. (1998) and da Silva et al. (2007). The WMS has a grid of 24 × 24 measurement points evenly distributed across the pipe cross-section given by a 24 × 24 wire configuration in two planes. It is based on capacitance measurements and is suitable for non-conductive materials such as oil. Fig. 2 shows a schematic diagram of the top view of the wire mesh sensor.

The two-phase mixture employed is air–silicone oil. The liquid has a surface tension about one third that of water and a viscosity of ~5 × water. The physical properties of the air–silicone oil system used are given in Table 1. In the interest of greater generality and compactness, the relevant dimensionless numbers in this experimental work are the Reynolds, Eötvös and Fr number, whose values are also reported in Table 1.

The experimental data were gathered in two campaigns: In the first campaign, the rig pipe inclination was set to simulate the flow of an air–silicone oil mixture up a vertical riser pipe. The measurements recorded by both the capacitance WMS and a pair of ECT probes were processed to obtain the structure velocity, as reported by Hernandez-Perez et al. (2010), Abdulkadir et al. (2014a, 2016). In the second campaign, the rig pipe inclination was set to horizontal and resultant air–silicone oil flows, were measured using the WMS and an ECT, as described by Abdulkareem et al. (2011). The transparent test pipe is 6 m long and 67 mm diameter. In both campaigns, the WMS was located at a distance 4.92 m upstream of the mixing or inlet section. The twin-plane ECT sensors were located at a distance of 4.4 and 4.489 m upstream of the air–silicone oil mixer injection portal located at the base of the vertical or horizontal pipe. The range of flow conditions studied during both campaigns, as characterized by the superficial velocities were: for air flow rates ranging from 0.05 to 4.72 m/s and for liquid flow rates (silicone oil) from between 0.05 m/s and 0.38 m/s. The measurement data were recorded at a data acquisition frequency of 1000 Hz over an interval of 60 s for the WMS and 200 Hz for the ECT. In addition, a high-speed video system was used to capture real time images of the flow regimes observed within the inclined pipe section under the different flow conditions (see Table 2).

Since density is affected by pressure fluctuations along the length of the pipe, it was necessary to correct the gas superficial velocity as a consequence of variations in pressure. Using the error analysis, the uncertainties in gas superficial velocities were determined and plotted in Fig. 3 for (a) vertical and (b) horizontal two-phase flows. It can be observed from the figure that the uncertainties changed based on flow conditions and pipe inclination and the uncertainties presented in Table 2 summarizes the minimum to

Table 1
Properties of the fluids and dimensionless numbers.

Fluid	Density (kg/m^3)	Viscosity (kg/ms)	Surface tension (N/m)
Air	1.224	0.000018	0.072
Water	1000	0.001	
Silicone oil	900	0.005	0.02
Dimensionless numbers			
Reynolds number for liquid, $\mathrm{Re}_L = \frac{U_{SL}\rho_L D}{\mu_L}$	603–4583		
Reynolds number for gas, $\mathrm{Re}_G = \frac{U_{SG}\rho_G D}{\mu_G}$	228–21,504		
Eötvös number, $Eo = \frac{(\rho_L-\rho_G)gD}{\sigma}$	1980		
Froude number for liquid, $Fr_L = \frac{U_{SL}^2}{gD}$	0.0038–0.22		
Froude number for gas, $Fr_G = \frac{U_{SG}^2}{gD}$	0.0038–34		

Table 2
Measurement uncertainties associated with gas superficial velocity, void fraction and temperature.

Quantity	Pipe inclination	Uncertainty
Gas superficial velocity (m/s)	Vertical	±7–22%
Gas superficial velocity (m/s)	Horizontal	±0.2–16%
Temperature		±0.2 °C
Liquid holdup from ECT		±5–7%
Void fraction from WMS		±3–5%

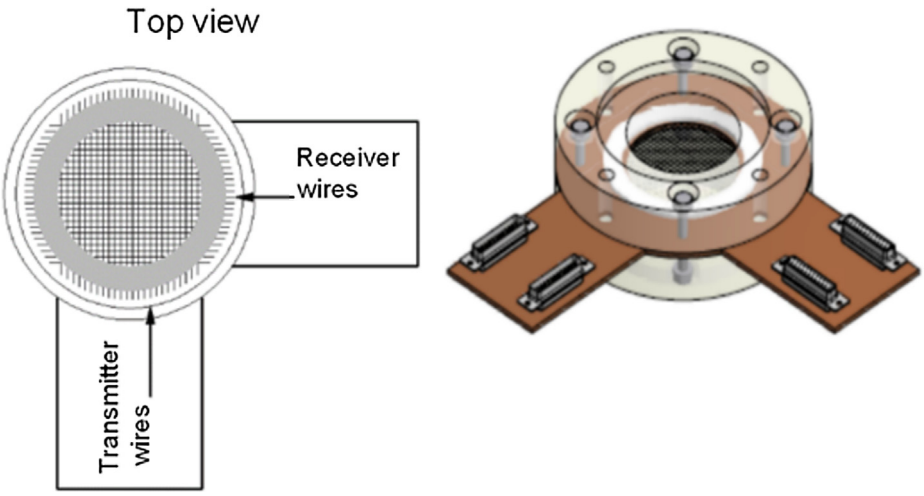

Fig. 2. Wire mesh sensor (WMS) (2 × 24 Electrode wires).

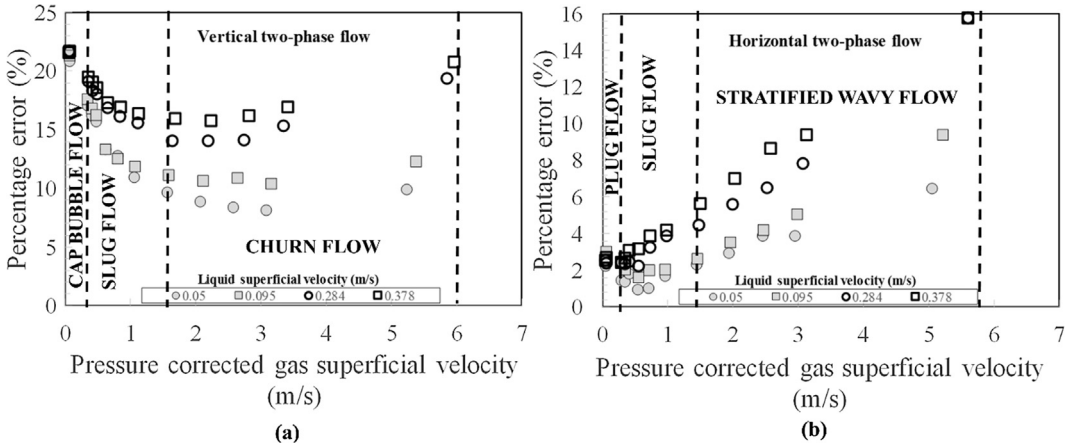

Fig. 3. Measurement uncertainties associated with gas superficial velocity for (a) vertical and (b) horizontal two-phase flows.

maximum ranges. Other important uncertainties associated with temperature, liquid holdup from the ECT and void fraction from the WMS are also presented in Table 2.

3. Discussion of results

3.1. Flow pattern map

To analyze, the measurement data recorded, 65 vertical and 65 horizontal two-phase air–silicone oil gas and liquid superficial velocities data points are plotted on a Pereyra and Torres (2005) flow pattern map to discern between the various flow patterns experienced in vertical and horizontal pipes. Fig. 4 therefore shows the flow pattern maps generated for air–silicone oil flows with the operating points showing the various flow patterns obtained in the present study for the (a) vertical and (b) horizontal pipe inclinations. The flow rates at which measurements were made for the vertical and horizontal flows are liquid and gas superficial velocities of (0.05–0.38) m/s and (0.05–4.72) m/s, respectively. From an analysis of the figures it may be concluded that for the vertical pipe, spherical cap bubble, slug and churn flow patterns were observed, whereas plug, slug and stratified wavy two-phase flow patterns are identified for the horizontal pipe (see Fig. 4).

3.2. Flow development

A fully developed flow according to Abdulkadir et al. (2015) is a scenario whereby the flow pattern does not change with the distance downstream. Flow development in the vertical and horizontal pipes was studied using ECT and WMS and the results are presented and discussed here. It is worth mentioning that the flow pattern often depends upon the observation position along the test section. This has given rise to the idea of partially and fully developed flow regimes. According to Abdulkadir et al. (2013, 2015), the extent to which a compressible gas flowing with an incompressible liquid in vertical and horizontal pipes can ever be considered fully developed is debatable. Also, due to physical limitations in the length of the rig, the question begging for an answer that we are going to address here is whether a sufficient pipe length had been provided so that observations taken at the end of the pipe could be considered to be a true representation of a fully developed flow situation.

Probability density function (PDF) of void fraction obtained from the ECT and WMS outputs are used to assess the change in flow characteristics with distance. The void fraction from the ECT for the vertical and horizontal pipes were obtained at locations of 4.4 and 4.489 m while 4.92 m for the WMS. Fig. 6 shows the results of flow development using PDF of void fraction derived from the three measurement locations for the vertical pipe at liquid and gas superficial velocities of 0.38 m/s and 0.05–4.72 m/s, respectively. On the other hand, Fig. 7 depicts similar scenario but for a horizontal pipe.

Fig. 5 shows the schematic diagram of the vertical and horizontal pipes including their corresponding measurement stations, ECT 1, ECT 2 and WMS. It is worthy of mention that at a distance of 4.4–4.92 m as depicted in Fig. 6, the PDF of void fraction at locations of

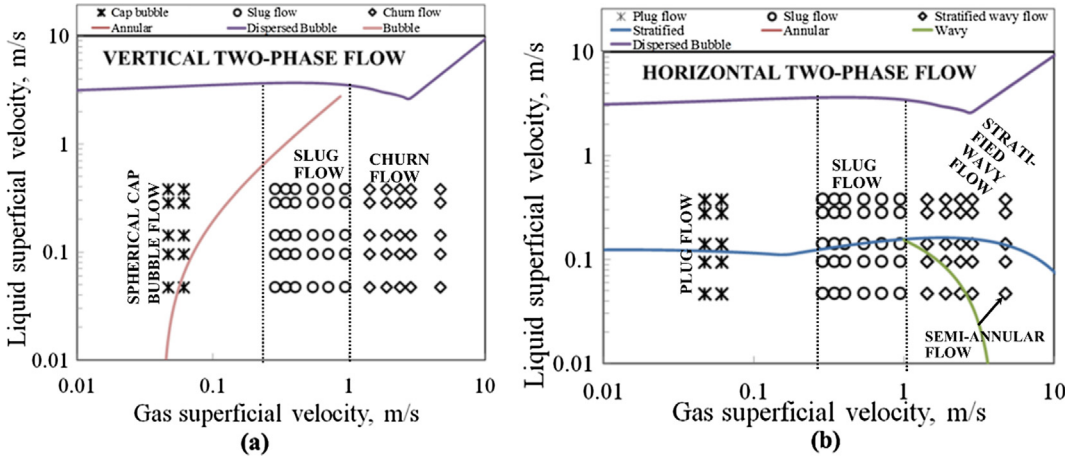

Fig. 4. Pereyra and Torres (2005) flow pattern map showing the positions of experimental points of consideration experienced in (a) vertical and (b) horizontal two-phase flows using air–silicone oil as the working fluid.

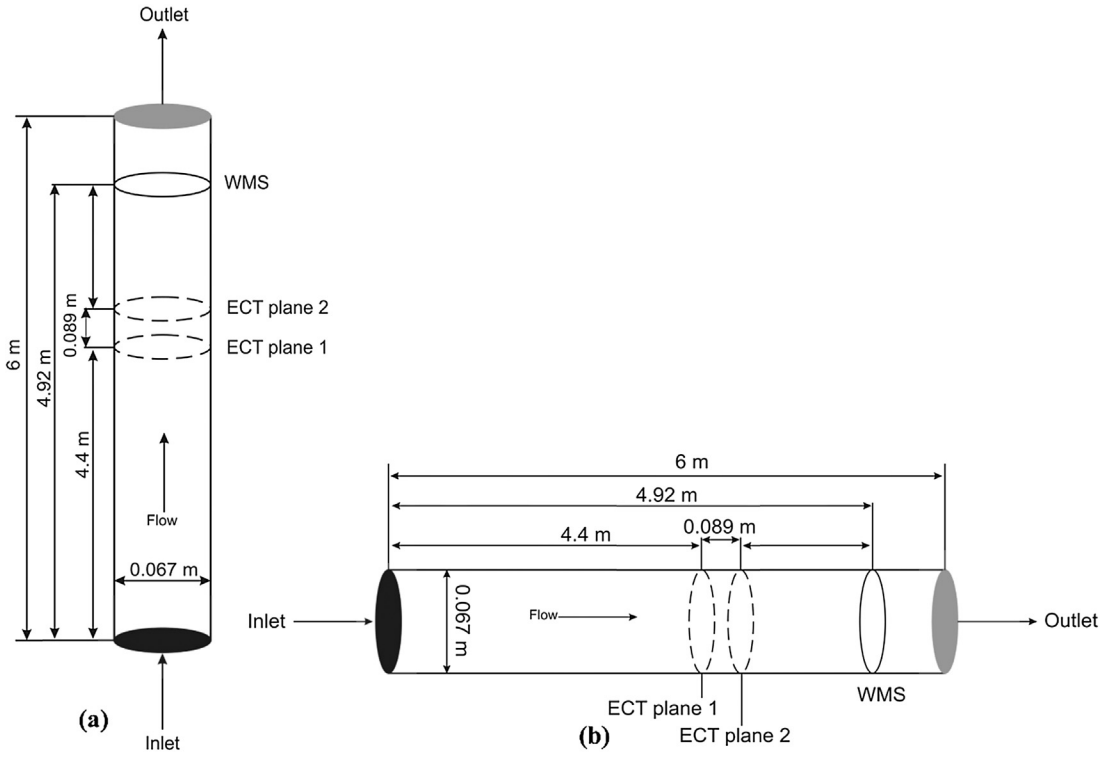

Fig. 5. Geometry of the (a) vertical and (b) horizontal pipes showing the locations of the measuring instruments.

ECT 1, ECT 2 and WMS all show the traditional features of spherical cap bubble, slug and churn flows. It is spherical cap bubble, Fig. 6 (a) and (b) because it presents a single peak of void fraction with a broadening tail extending to a higher values. On the other hand, the presence of a double peak, Fig. 6(c)–(e) corresponds to slug flow; one peak at lower void fraction represents liquid slug whilst the one at higher void fraction, Taylor bubble. Fig. 6(f) and (h) shows a single peak at high void fraction ($\varepsilon \geqslant 0.74$) with broadened tails down to lower void fractions. This is a typical feature of churn flow. It can be concluded therefore that between, 4.4–4.92 m, that the flow is fully developed and statistically stable based on the fact that the flow remains quite similar, i.e. not changing with distance. This corresponds to approximately 66–73 pipe diameters.

On the matter of horizontal flow, at a distance of 4.4–4.92 m as depicted in Fig. 7, the ensuing flow patterns are plug, slug and stratified wavy flows. It is worthy of mention that the observed flow patterns from the three measuring stations are not the traditional plug, slug and stratified wavy flows, they do not exactly reflect the characteristic signatures of the flow patterns under consideration. It can be concluded based on the PDF of void fraction that the flow patterns recorded at ECT 1, ECT 2 and WMS are partially developed based on the fact that the flow patterns at ECT 1 (4.4 m) and ECT 2 (4.489 m) are quite similar but slightly different from at WMS (4.92 m).

It is worth mentioning that given that the pressure gradient is dependent on the flow pattern, flow development from the pressure gradient's perspective is expected to be the same.

3.3. Reconstructed images of two-phase flow pattern obtained from WMS

Figs. 8 and 9 present visualization of the cross sectional or reconstructed images of vertical and horizontal two phase flows produced by processing of the measurement data recorded by the WMS at liquid and gas superficial velocities of 0.38 m/s and 0.05–4.72 m/s, respectively. The methodology for processing the raw WMS data is as follows: for each run, a raw data file is obtained from the WMS. It contains a matrix of 24 × 24 for every 1/1000 of a second in the form of a 3D array of void fractions, α (i, j, k), where k is the number of measurements, i and j correspond to a pair of crossing electrode wires (transmitter and receiver). The file is then read in the processing software, such as Matlab. To construct the images of the axial slides views, the data corresponding to a central plane, α (i, 12, k), are plotted as an image. The pure gas and liquid phases are red and blue, respectively.

In Fig. 8, the reconstructed images of two-phase flow patterns for the vertical pipe are compared against that for the horizontal pipe, Fig. 9 at the same flow conditions. Fig. 8 presents the side views of the vertical two-phase flows produced by processing the measurement data recorded by the WMS.

The figure gives considerable insight into the phase distributions within the air–silicone oil flows. At a liquid superficial velocity of 0.38 m/s, there are small individual gas bubbles, usually in clusters, arriving at the WMS measuring station. With an increase in gas superficial velocity, the bubbles in form of clusters are observed to have coalesced into large bubbles, occupying most of the pipe cross-section. However, these larger bubbles do not have the typical bullet shape; the so-called Taylor bubbles. Kataoka and Ishii (1987) experimentally verified that for the motion of gas bubbles through non-dimensional pipe diameter (D^*), a typical Taylor bubble cannot exist when the calculated D^* according to Eq. (1) is greater than 40. Given that for the experimental rig used for this study $D^* = 45$, a bullet-shaped Taylor bubble is not expected. Indeed, for such a large pipe diameter, the gas bubbles tend to grow in a lateral direction as compared to their growth in longitudinal direction for relatively small pipe diameters.

$$D^* = \frac{D}{\sqrt{\frac{\sigma}{g\Delta\rho}}} = 45 \tag{1}$$

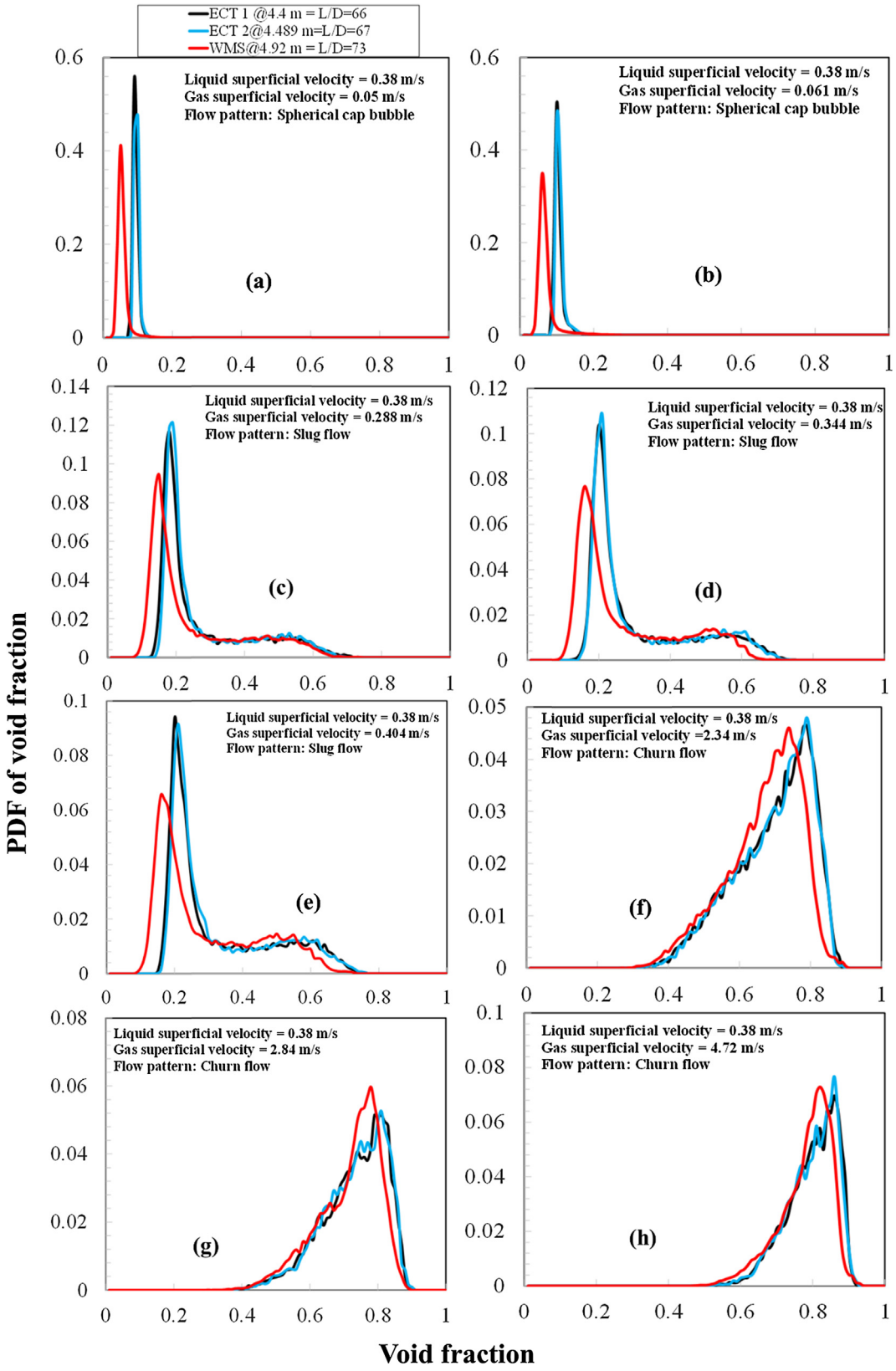

Fig. 6. Flow development in a vertical 67 mm internal diameter and 6 m long pipe using PDF of void fraction at various liquid and gas superficial velocities. The measuring instruments used are electrical capacitance tomography (ECT) and wire mesh sensor (WMS). The ECT and WMS locations as shown in Fig. 5 are: ECT plane 1 at 4.4 m, ECT plane 2 at 4.489 m and WMS at 4.92 m.

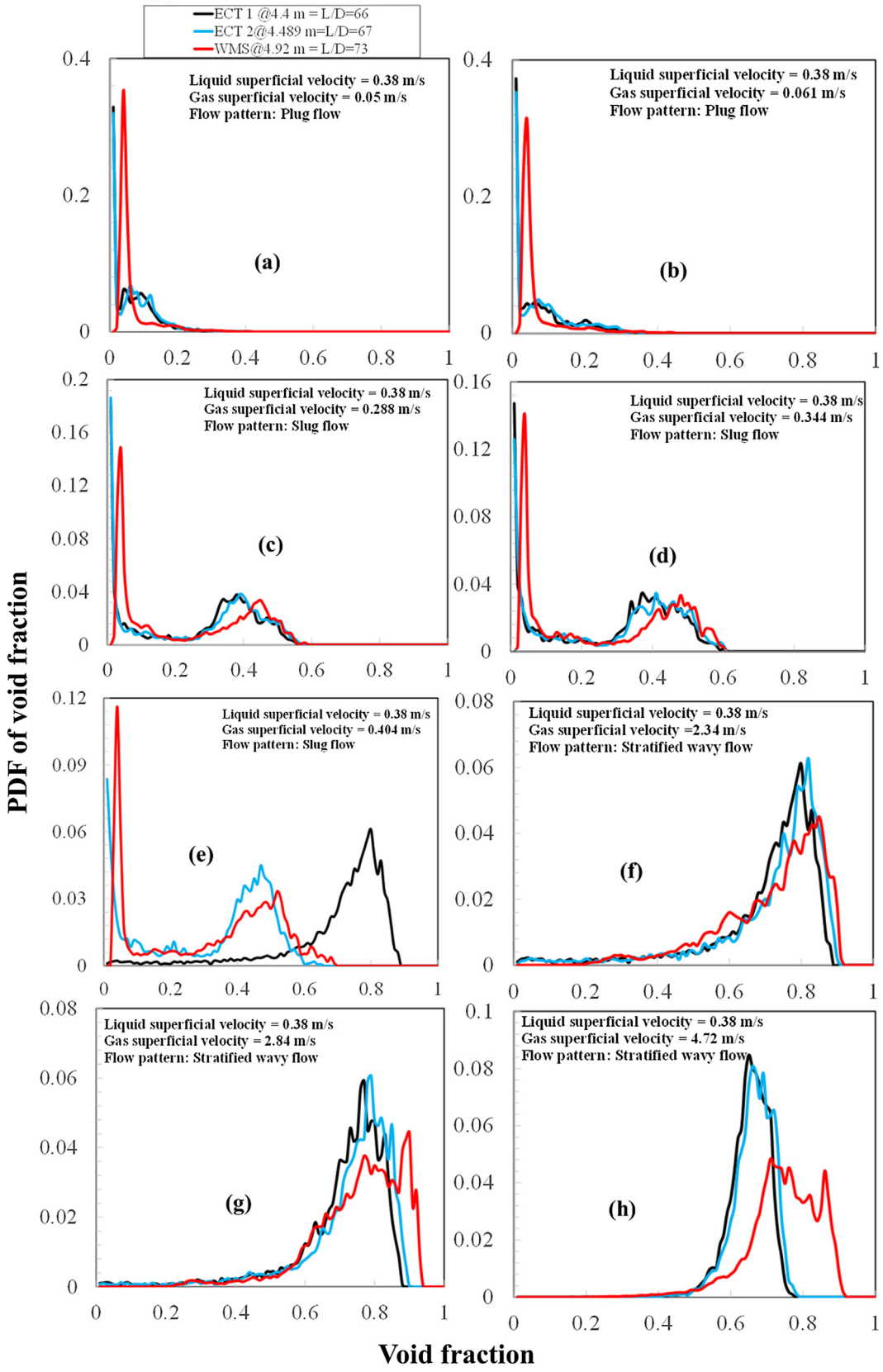

Fig. 7. Flow development in a horizontal 67 mm internal diameter and 6 m long pipe using PDF of void fraction at various liquid and gas superficial velocities. The measuring instruments used are electrical capacitance tomography (ECT) and wire mesh sensor (WMS). The ECT and WMS locations as shown in Fig. 5 are: ECT plane 1 at 4.4 m, ECT plane 2 at 4.489 m and WMS at 4.92 m.

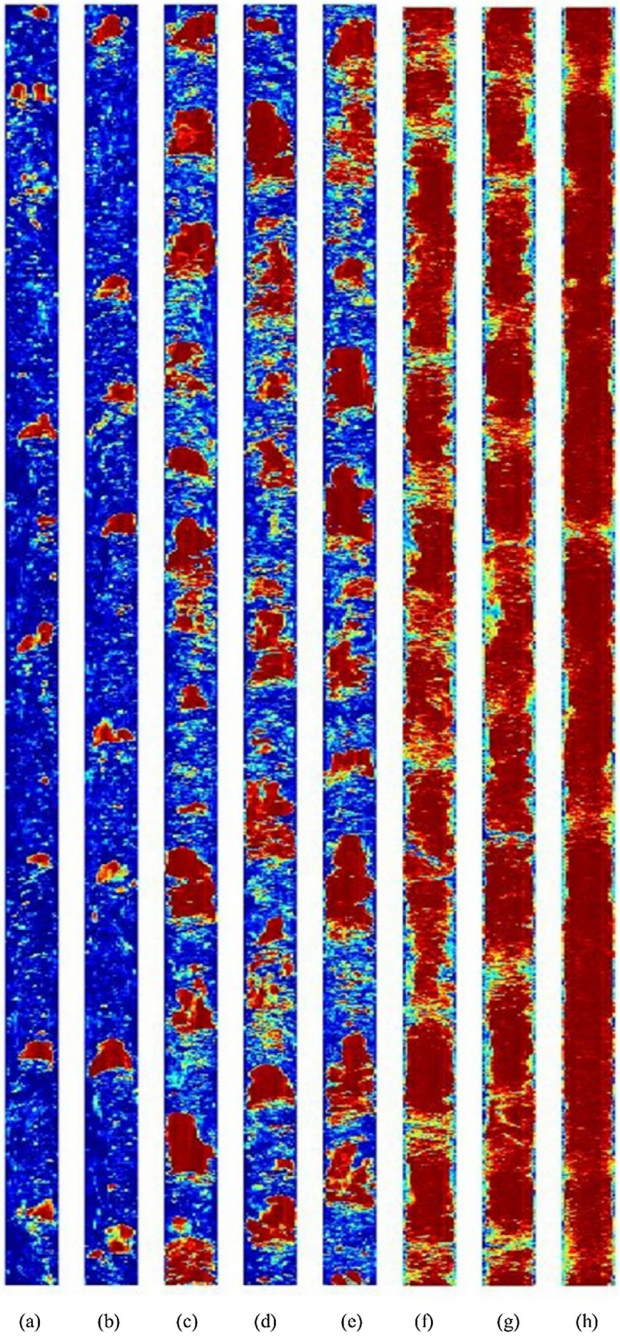

Fig. 8. Reconstructed images of two-phase flow pattern for the vertical pipe at liquid superficial velocity of 0.38 m/s and at gas superficial velocity (m/s) of (a) 0.05 (b) 0.061 (c) 0.288 (d) 0.344 (e) 0.404 (f) 2.36 (g) 2.84 and (h) 4.72.

where $D^*, \sigma, g, \Delta\rho$ represent, the non-dimensional diameter value, liquid surface tension, gravitational acceleration and density difference, respectively.

At gas superficial velocities of between 1.42 and 4.72 m/s, periodic structures with high liquid contents can be seen.

On the other hand, Fig. 9 presents an examination of the virtual side views of the flow phases determined from a processing of the WMS measurement data for the flows observed in horizontal air–silicone oil mixtures. At liquid and gas superficial velocities of 0.38 m/s and 0.05 m/s, respectively, the flow pattern is plug flow. For higher flow velocities, where shear forces are dominant, waves are formed at the gas–liquid interface. This is due to the influence of gravity on the fluid distribution to separate the liquid to the bottom of the pipe and the gas to the top. For higher liquid, slug flow pattern is observed. The elongated bubbles between the liquid slugs are observed to grow as gas superficial velocity increases.

3.4. Variation of time averaged void fraction with gas superficial velocity

A comparative analysis of the effects that changes in the liquid and gas superficial velocities have on the observed average void fractions for the vertical and horizontal pipe orientations respectively, are presented on Fig. 10.

From an analysis of Fig. 10, it is concluded that there is a noticeable difference in the average void fractions observed between the horizontal and vertical pipe configurations. The difference is higher at the minimum gas and liquid superficial velocities, both of 0.05 m/s, with the horizontal pipe having higher values. This behaviour might be expected as in horizontal two-phase flow, this results in a stratified flow, where the liquid phase tends to move against friction force only, whilst for a vertical two-phase flow the liquid phase will undergo both friction and gravitational forces opposite the flow. These competing processes cause the actual gas velocity to be greater in vertical two-phase flow than in the corresponding horizontal configuration. Therefore, for the same liquid and gas superficial velocities, higher values of void fraction are observed for horizontal two-phase flows due to the higher residence time of the gas phase within the test pipe section. At a gas superficial velocity 4.72 m/s, the values of the observed vertical and horizontal void fractions for the two pipe configurations become almost equal. This is not surprising because under these conditions, the flow patterns observed within the vertical and horizontal pipes are similar.

However, as the liquid superficial velocity gradually increases from 0.095 to 0.38 m/s, the observed systematic divergence tends to reduce as the liquid superficial velocity increases. At high gas superficial velocities, the void fractions are almost identical, which also indicates similar phase velocities. This is because under these conditions, the inertial forces become dominant with respect to gravity forces, Fr number = 6.74. Therefore, void fraction, tends to become independent of pipe orientation.

3.5. Variation of frequency with gas superficial velocity

Intermittent flow is characterized by a variation of the observed void fraction with time, mainly in the form of periodic structures. To characterize these structures, an analysis of the fluctuations observed in the void fraction time series was conducted to determine its frequency, by employing the Power Spectral Density (PSD) method, detailed in Abdulkadir et al. (2014b). Fig. 11 shows a comparison between the determined vertical and horizontal frequencies. From an analysis of the data plots, the vertical two-phase flow frequency is observed to be greater than that observed for the horizontal pipe configuration at the same liquid and gas superficial velocities. This increase in observed frequency between the two cases is to be expected as, due to the action of gravity that produces more liquid accumulation. Consequently, the frequency of the flows associated with the vertical pipe are greater. It is also observed that the frequencies initially rise and fall as the gas superficial velocity increases, particularly for the vertical case. This observed rise and fall in frequency might be associated with an observed coalescence of bubbles and the attendant observed changes in the flow pattern associated with a change in the liquid superficial velocity. In addition, some observed frequencies in the horizontal two-phase flow are associated with separated flows, stratified wavy flow. This is in agreement with the observations of Hubbard and Dukler (1966) who reported that for separated flows, stratified and stratified wavy flows, the frequency is zero.

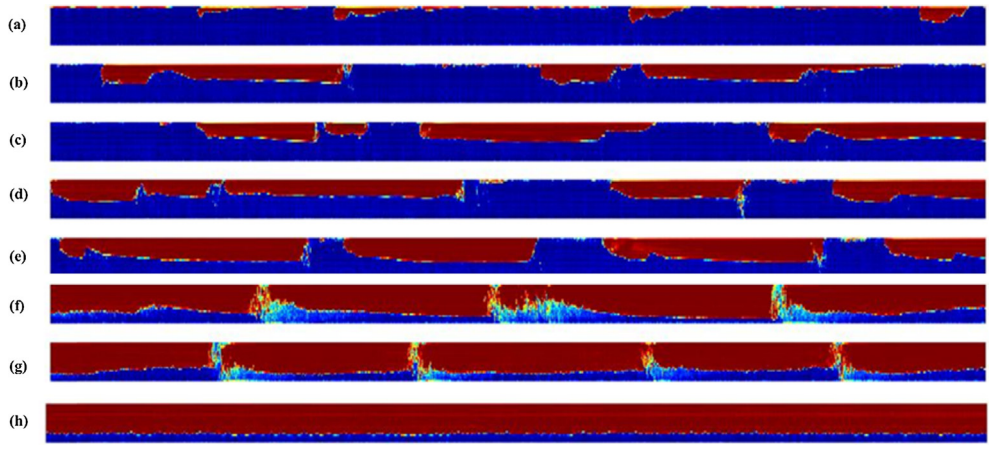

Fig. 9. Reconstructed images of two-phase flow pattern for the horizontal pipe at liquid superficial velocity of 0.38 m/s and at gas superficial velocity (m/s) of (a) 0.05 (b) 0.061 (c) 0.288 (d) 0.344 (e) 0.404 (f) 2.36 (g) 2.84 and (h) 4.72.

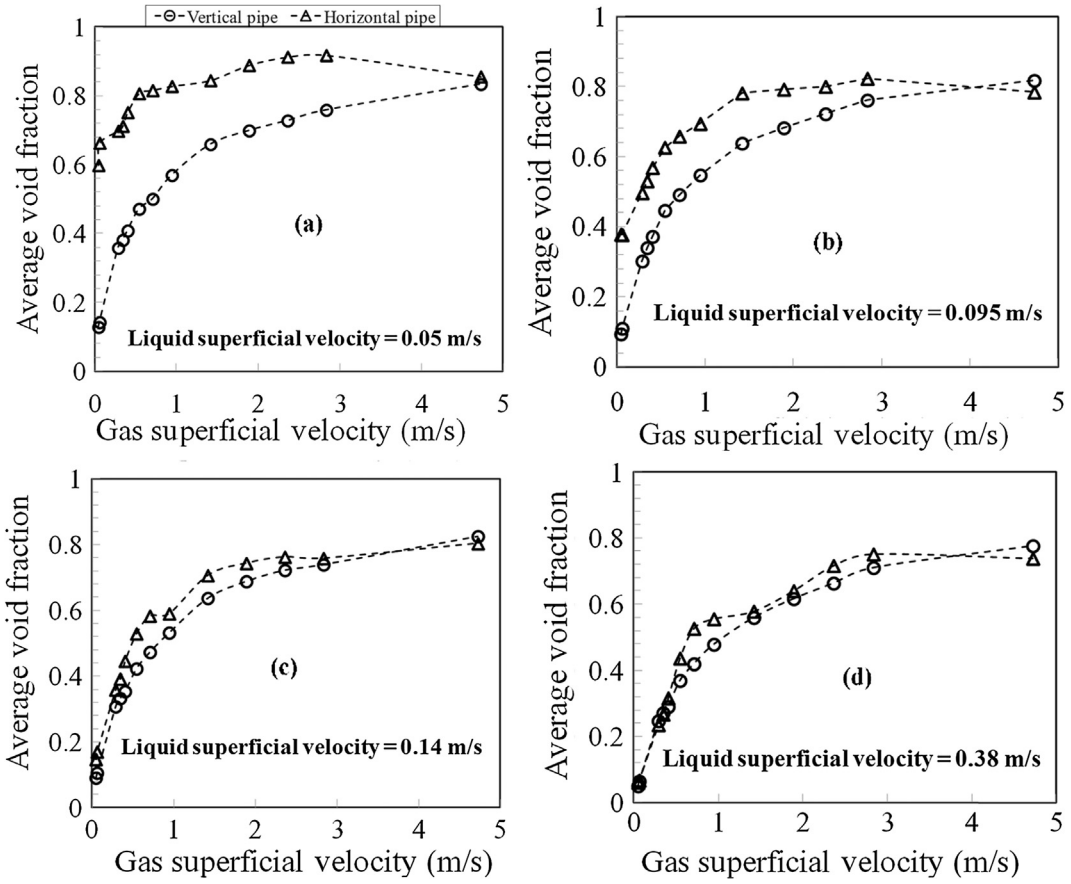

Fig. 10. Effect of gas superficial velocity on time averaged void fraction experienced in vertical and horizontal two-phase flows at liquid and gas superficial velocities of (0.05–0.38) m/s and (0.05–4.72) m/s, respectively.

3.6. Structure (bubble) translational velocity

Cross-correlation of the time series of void fraction determined by the two ECT probes allows the structure (translational) velocity of the observed flow patterns to be determined. The details of the cross-correlation method can be found in Abdulkadir et al. (2014b).

(a) Comparison between structure velocities determined from vertical two-phase flow against structure velocity determined from horizontal two-phase flow

Fig. 12 shows the comparison between the structure velocity of the bubble concerned with vertical and horizontal two-phase flows. The values were calculated by cross-correlating the signals from two ECT probes located 89 mm apart. The figure shows a comparison of structure velocity at liquid and mixture superficial velocities of (0.05–0.38) m/s and (0.1–6.0) m/s, respectively, for vertical and horizontal two-phase flows.

There is a significant difference in the magnitude of the structure velocity observed at the highest gas superficial velocity of 4.72 m/s for all the liquid superficial velocities considered, with the vertical

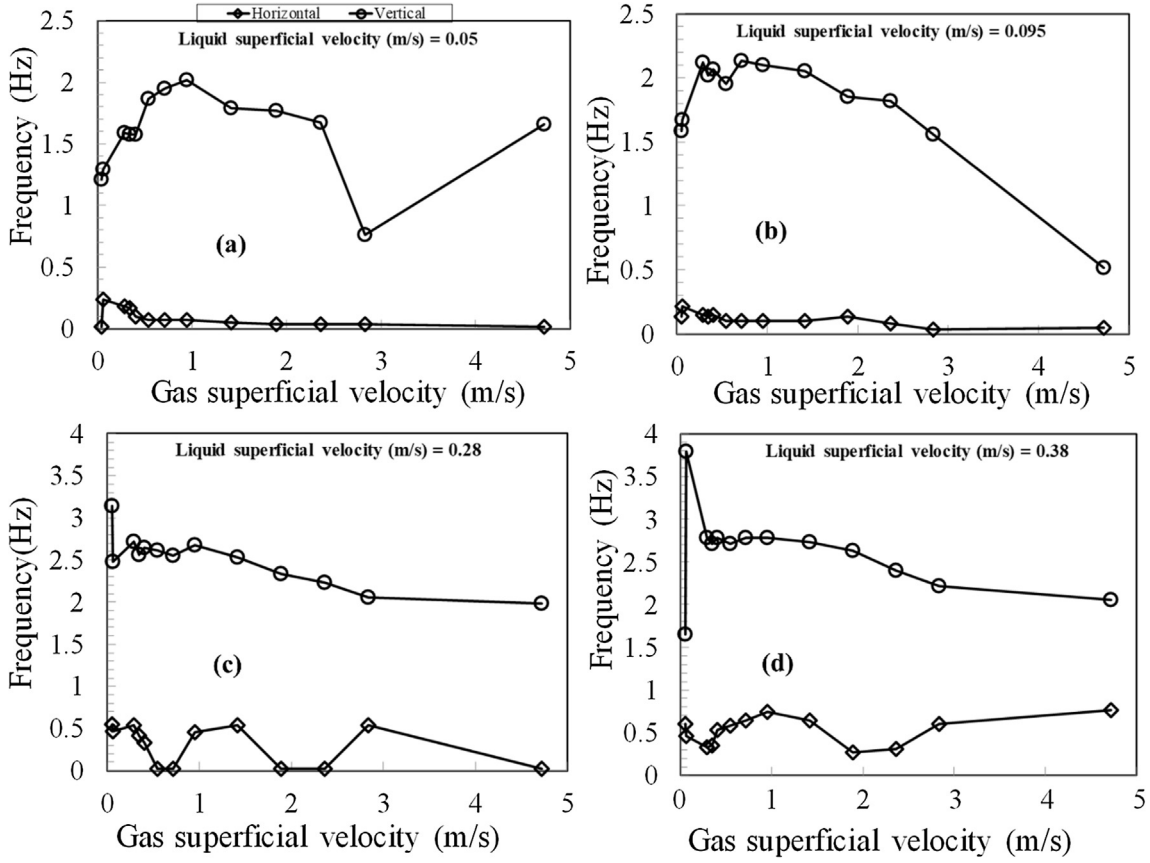

Fig. 11. Variation of frequency with gas superficial velocity at liquid superficial velocity (m/s) of (a) 0.05 (b) 0.095 (c) 0.28 and (d) 0.38.

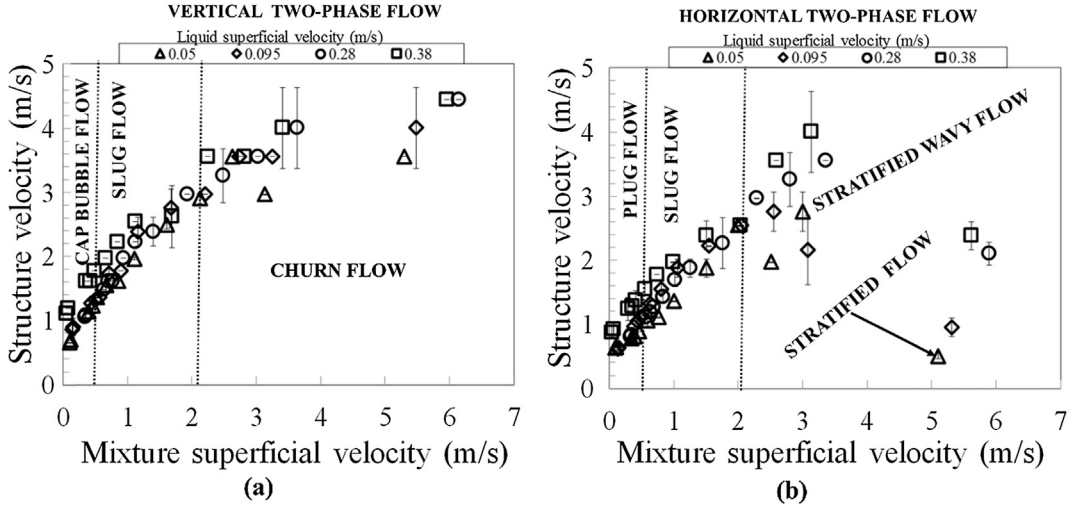

Fig. 12. Structure velocity comparison between (a) vertical and (b) horizontal two-phase flow. The bar represents standard deviation.

two-phase flow having a higher value. This could be related to the flow pattern transition that happens when the gas superficial velocity increases at a fixed liquid superficial velocity. In vertical flow, the flow pattern changes from slug to churn, whereas in horizontal it changes from slug to semi-annular flow. It can be deduced that the respective flow pattern transition occurs earlier for the horizontal or simply that huge waves in churn flow travel faster than horizontal waves in semi-annular flow. In addition, some fluctuations are observed in the data, for both the vertical and horizontal two-phase flows, which can be attributed to uncertainties.

For vertical two-phase flows, the structure velocity as depicted in Fig. 12(a) can be observed to increase with an increase in mixture superficial velocity for all the liquid superficial velocities considered. It can also be observed from the plot that the liquid superficial velocity has an insignificant effect on the structure velocity. Identical structure velocities in some cases can be observed for reason of same flow pattern and same phase velocity. In addition, the structure velocity though not quite significant can be observed to be higher for the vertical two-phase flow. On the other hand, for the horizontal two-phase flow, Fig. 12(b), the struc-

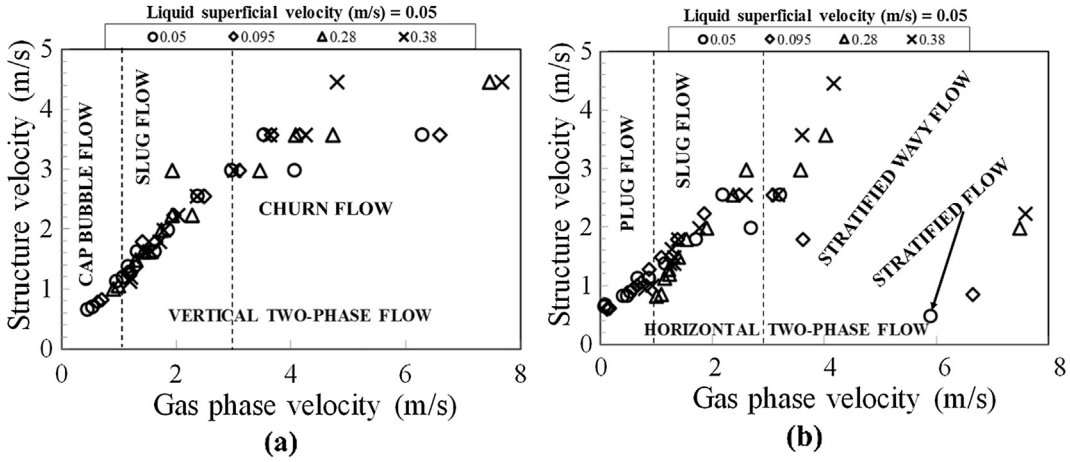

Fig. 13. Relation between structure velocity and gas phase velocity for (a) vertical and (b) horizontal two-phase flow.

ture velocity can be observed to increase and then decrease with an increase in mixture superficial velocity for the same flow conditions considered for the vertical two-phase flow. In addition, some of the observed fluctuations in some values of the structure velocity in particular with regards to slug flow can be attributed to the fact that the flow is partially developed.

(b) Structure velocity against gas velocity for vertical and horizontal two-phase flows

For the plot of structure velocity against gas phase velocity, Fig. 13(a) and (b), a similar trend that was observed in Fig. 12(a) and (b) is also seen here. The plot corroborates the observations in Fig. 12(a) and (b) that the liquid superficial velocity has an insignificant effect on structure velocity. An increase in structure velocity can be observed as the gas phase velocity increases for the liquid superficial velocities considered. At gas phase velocity of $1 \leqslant U_G \leqslant 3$ m/s, the corresponding flow pattern for both the vertical and horizontal two-phase flows is slug flow and the structure velocities are generally almost identical. The structure velocities are almost identical for 2 likely reasons: (1) Similar flow pattern and (2) identical phase velocities as a consequence of similar void fractions in both the vertical and horizontal pipes.

It is worth mentioning that for churn flow, which occurs in vertical flow, the structures are called huge waves. These can be observed in Fig. 8(f), (g), and (h). They occur when the liquid slug body becomes unstable, leading to break-up and fall as gas superficial velocity increases. This liquid merges with the approaching slug, which then resumes its upward motion until it becomes unstable and after which it falls once again. As a result, the structure velocity decreases followed by an increase, as illustrated in Figs. 12(a) and 13(a). Similarly, for stratified wavy flow, which occurs in horizontal flow, the structures consist of waves. Therefore, the physical meaning of the structure velocity that is calculated with the cross correlation is the velocity of the waves. The waves are often classified into 2-D waves and Kelvin-Helmholtz (KH) waves, also called pseudo-slugs. These can be observed in Fig. 9(f) and (g). They occur when the liquid slug body becomes aerated. As illustrated in Fig. 12(b) and 13(b), the structure velocity increases followed by a considerable decrease as the gas velocity increases.

3.7. Drift-flux parameters

The drift-flux model proposed by Zuber and Findlay (1965) can be used to calculate void fraction. It correlates the actual gas velocity, V_G, and the mixture superficial velocity, U_M, using two drift-flux parameters, C_0 and V_D. This is represented in Eq. (2).

$$V_G = C_0 U_M + V_D \tag{2}$$

where U_M, C_0, and V_D are the mixture superficial velocity, distribution coefficient and drift velocity of gas, respectively.

The drift-flux model is one of the most practical and accurate models for two-phase flow analysis Weber (1981). The model considers the effects of non-uniform flow, void fraction profiles as well as the local relative velocity between both phases. A plot of V_G against U_M is presented in Figs. 14 and 15 for two-phase flow in vertical and horizontal pipe configurations, respectively. The plots represent all the individual flow patterns observed in both vertical and horizontal pipe configurations of two-phase flows in order to obtain their respective drift parameters. The individual plots show the determination of the corresponding drift flux parameters, C_0 and V_D as well as their corresponding correlation coefficient obtained for each of the flow patterns observed in both pipes.

Fig. 14 shows a plot of the computed mixture superficial velocity and gas velocities for two phase flows representing spherical cap bubble, slug and churn flows and the derivation of the corresponding drift flux parameters. It is noted that the actual gas velocity value at $U_M = 0$ m/s represents the drift velocity, whilst C_0 is the slope assumed to be constant for each of the flow patterns under consideration. From the plots, C_0 is estimated to be 2.52, 1.23 and 1.093 for spherical cap bubble, slug and churn flows, respectively. The drift velocity from the plot are determined to be 0.33, 0.70 and 0.52 m/s for spherical cap bubble, slug and churn flows, respectively. To compare these values, to those reported by similar studies reported in the literature, the drift velocity needs to be expressed as a function of drift parameter, i.e., $x\sqrt{gD}$, where x is the drift parameter. Thus, for spherical cap bubble, slug and churn flows, the estimated drift parameters are 0.40, 0.87 and 0.64, respectively. Nicklin et al. (1962) reports a comparative drift parameter value of 0.35 for an air–water slug flow in a vertical pipe.

The velocities concerned with the horizontal pipe configuration two-phase flow scenario are shown in Fig. 15. The drift-flux parameters for slug flow, shown in Fig. 15(a), are distinctly different from those shown for the (b) plug and (c) stratified wavy flows. From the plot, the estimated C_0 values for plug, slug and stratified wavy flows are 2.248, 1.246 and 1.214, respectively. These values of C_0 were obtained by curve fitting the experimental data with equation of straight line. These values are contrary to the observations reported by Franca and Lahey (1992) and Bhagwat and Ghajar

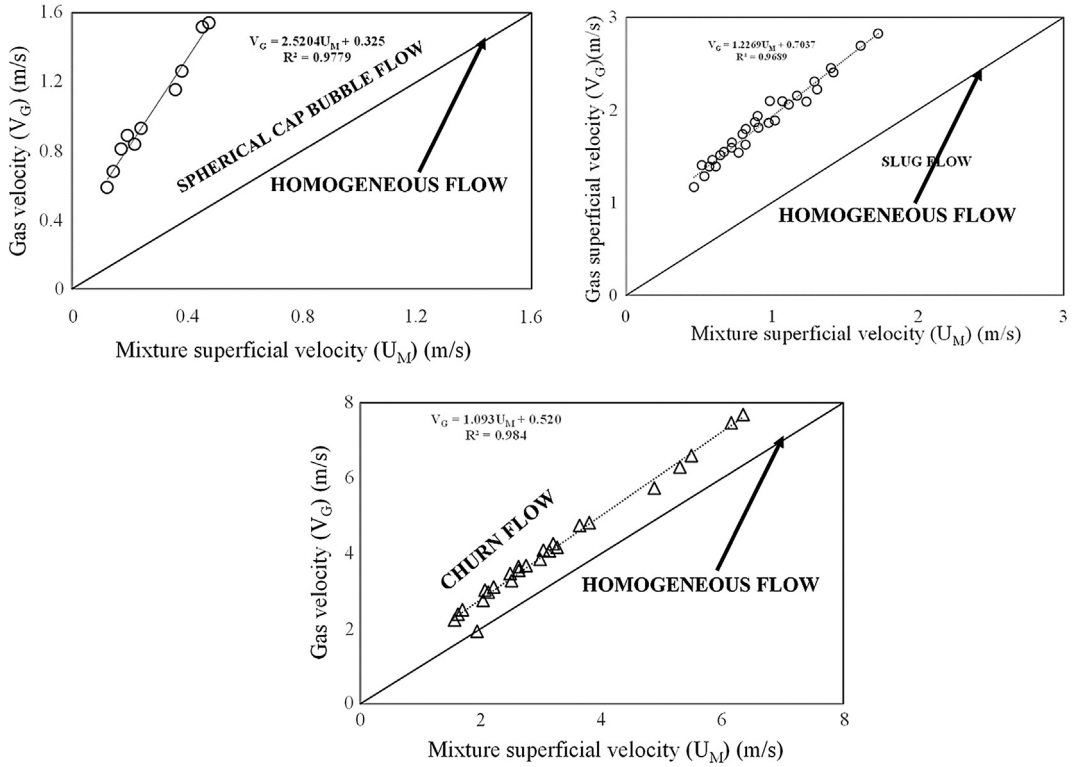

Fig. 14. Dependency of vertical two-phase flow gas velocity on mixture superficial velocity for (a) spherical cap bubble (b) slug (c) churn flows. Above the 45°-diagonal line, $U_G > U_L$ and hence $C_0 > 1$ and $V_D > 0$. On the 45°-diagonal line, $U_G = U_L$ and hence $C_0 = 1$ and $V_D = 0$, the flow is homogeneous. Below the 45°-diagonal line, $U_G < U_L$ and hence $C_0 < 1$ and $V_D < 0$.

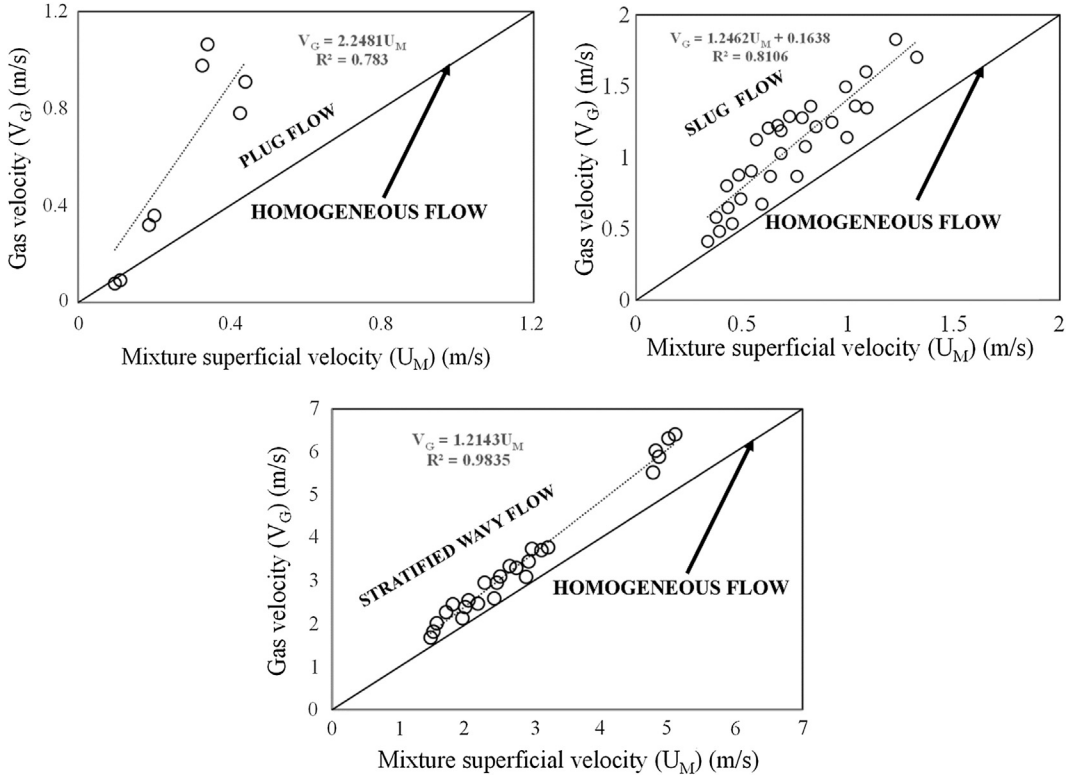

Fig. 15. Dependency of horizontal two-phase flow gas velocity on mixture superficial velocity for (a) plug (b) slug (c) stratified wavy flows. Above the 45°-diagonal line, $U_G > U_L$ and hence $C_0 > 1$ and $V_D > 0$. On the 45°-diagonal line, $U_G = U_L$ and hence $C_0 = 1$ and $V_D = 0$, the flow is homogeneous. Below the 45°-diagonal line, $U_G < U_L$ and hence $C_0 < 1$ and $V_D < 0$.

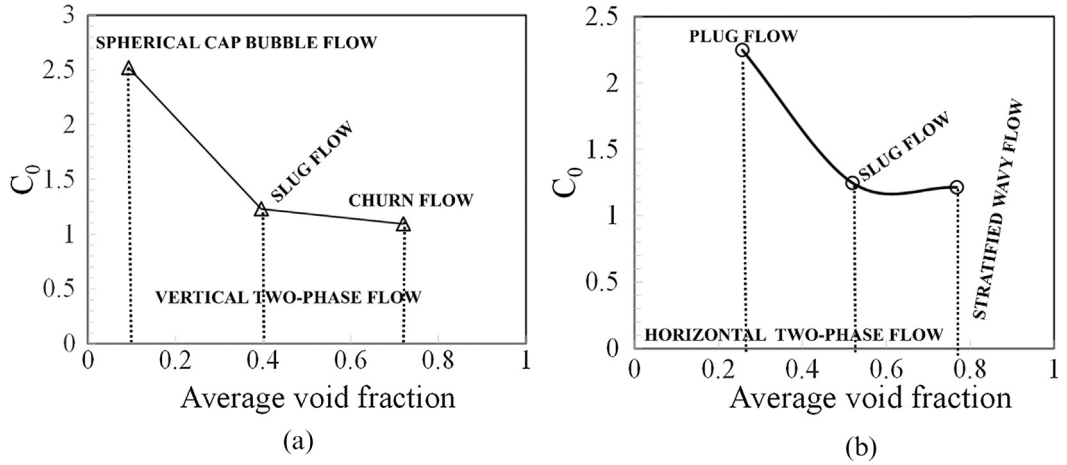

Fig. 16. Dependency of distribution coefficient, C_0, with average void fraction in (a) vertical and (b) horizontal two-phase flows.

(2014). Franca and Lahey (1992) found that for low values of gas flow rates in horizontal flow, C_0 is close to unity. Bhagwat and Ghajar (2014) on the other hand found that in case of bubbly and slug flow in horizontal pipe that the value of C_0 is between 1 and 1.1. Interestingly, Gokcal (2006) experimentally determined C_0 for slug flow using highly viscous liquids and found that unlike the value of C_0 in a range of 1.1 and 1.2 in air–water two-phase slug flow, liquid of high viscosity can cause the value of C_0 to go as high as 2.0. This large variation in parameter value proposed by Gokcal (2006) is probably due to the laminarization of the two-phase flow. The computed drift velocity values are 0, 0.163 and 0 m/s for plug, slug and stratified wavy flows, respectively. The corresponding drift parameters for the three flow patterns are 0, 0.201 and 0. The observed zero values for the drift velocity for two of the flow patterns imply that the local relative velocity is zero. Wallis (1969), Dukler and Hubbard (1984) as well as Bonnecaze et al. (1971) claimed that the drift velocity is zero for the horizontal case since the buoyancy force does not act in the flow direction. In addition, the higher values of C_0 according to Franca and Lahey (1992) may be attributed to the displacement experienced by the gas bubbles, its expansion due to a higher pressure drop and the liquid velocity distribution in the flow patterns. Bendiksen (1984), Nicholson et al. (1978) and others showed that a drift velocity exists for the horizontal case and that in fact it may even exceed its value in the vertical case. It may be concluded that for horizontal two-phase slug flow that the drift velocity is not normally zero. Thus, the conclusions of this study also confirm the findings of Weber (1981), Nicholson et al. (1978) and Benjamin (1968), who reported that drift velocity exists in horizontal flows because of the balance between lateral and axial pressure gradients. It also confirms the reported linear relationship between V_G and U_M for all the considered flow patterns in the present work regardless of the pipe inclination.

3.7.1. Distribution coefficient, C_0, and drift velocity, V_D

Figs. 16 and 17 show a plot of the parameter values C_0 and V_D, respectively, against average void fraction determined at different liquid and gas superficial velocities for vertical and horizontal two-phase flows.

(a) Distribution coefficient, C_0

Fig. 16 shows that on the matter of vertical two-phase flow, spherical cap bubble is established at low void fraction of between 0.07 and 0.4 and corresponding high C_0 values of between 2.52 and 1.23.

For slug flow, average void fraction, ε, is between 0.4 and 0.7 while C_0 is between 1.23 and 1.09. At $\varepsilon \geqslant 0.75$ and $C_0 \leqslant 1.09$, churn flow is observed. This behaviour may be explained by a consideration of the phase concentration profiles in churn, slug and spherical cap bubbles. In churn flow, the overall gas distribution is uniform as a consequence of the presence of a few liquid

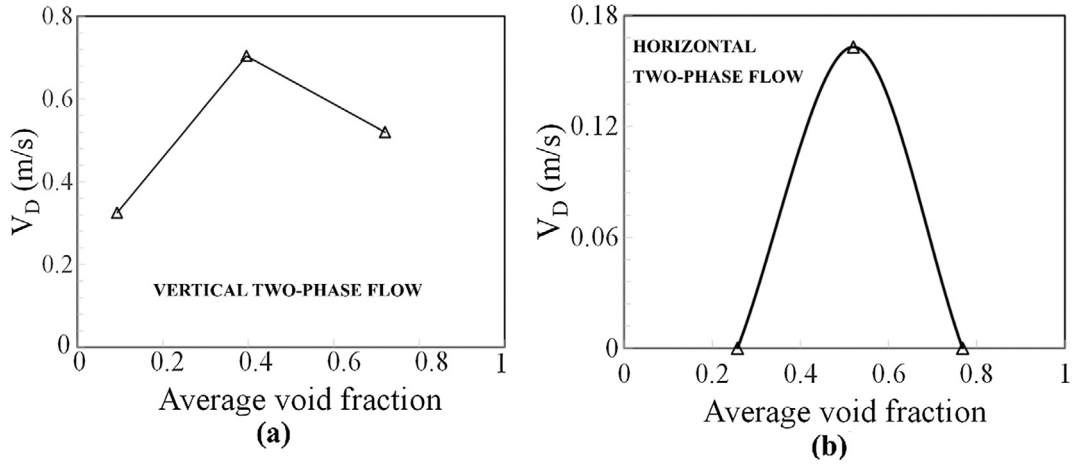

Fig. 17. Dependency of drift velocity, V_D, with average void fraction in (a) vertical and (b) horizontal two-phase flows.

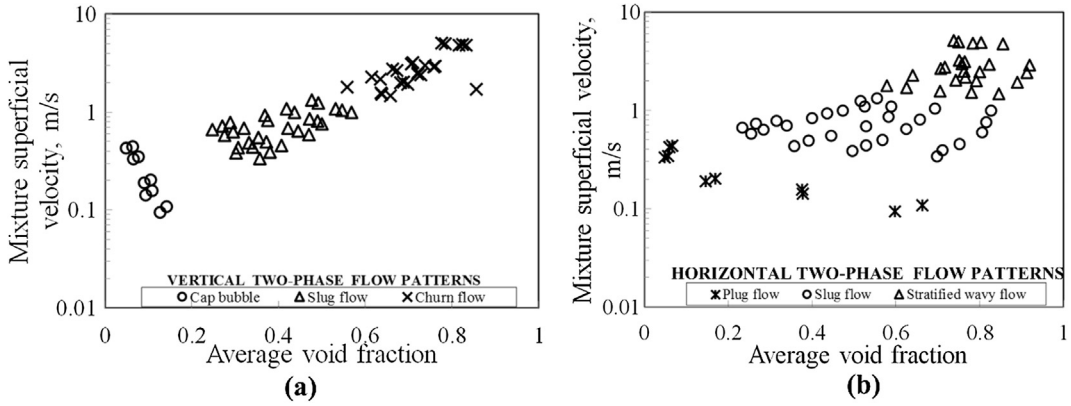

Fig. 18. Dependency of mixture superficial velocity on average void fraction for (a) vertical and (b) horizontal two-phase flows.

droplets entrained in the gas core, and as a result $C_0 \approx 1$. However, in slug flow, where Taylor bubbles and liquid slugs appear alternatively, $C_0 > 1$ since the non-uniform effects are strong. In spherical cap bubbles with a bubble size less than the pipe diameter, the non-uniform effects are much stronger and as a result $C_0 > 1.3$.

For the horizontal two-phase flow, Fig. 16(b), plug flow is seen at a C_0 value of between 2.248 and 1.246 at a corresponding average void fraction of 0.23–0.5. At $0.5 \leqslant \varepsilon \leqslant 0.75$ and $1.214 \leqslant C_0 \leqslant 1.246$, slug flow is observed. Stratified wavy flow is observed at $\varepsilon \leqslant 0.75$ and $C_0 \leqslant 1.214$.

(b) Drift velocity, V_D

Fig. 17(a) shows that the drift velocity in vertical two-phase flow increases with an increase in average void fraction.

Similarly, for horizontal two-phase flow, as depicted in Fig. 17 (b), the relationship between drift velocity and average void fraction is a bell-shaped curve, with the peak value depicting slug flow whilst the two lower ends represent plug and stratified wavy flows.

3.8. Determination of flow pattern map using variation of mixture superficial velocity with average void fraction

Fig. 18 presents a plot of the variation of mixture superficial velocity with average void fraction for various liquid and gas superficial velocities, for each of the vertical and horizontal pipe configurations.

Considering the vertical pipe configuration two-phase flow, Fig. 18(a), spherical cap bubble is observed at low void fraction and low mixture superficial velocity. As void fraction gradually increases from 0.25 to 0.65, slug flow is established. Churn flow is observed between void fractions $0.6 \leqslant \varepsilon \leqslant 0.85$. However, in Fig. 18(b) for the horizontal pipe configuration two-phase flow, plug flow is observed for void fractions between $0.02 \leqslant \varepsilon \leqslant 0.7$ and mixture superficial velocities of between $0.1 \leqslant U_M \leqslant 0.7$ m/s. Slug flow is created between $0.2 \leqslant \varepsilon \leqslant 0.82$ and $0.2 \leqslant U_M \leqslant 2$ m/s. At void fractions of between $0.5 \leqslant \varepsilon \leqslant 0.95$, stratified wavy flow is observed. Consequently, it is concluded that a plot of mixture superficial velocity against average void fraction may be used to provide a qualitative index of flow pattern.

4. Conclusion

Advanced instrumentation, electrical capacitance tomography (ECT) and wire mesh sensor (WMS) were used to detect the local instantaneous cross-sectional distribution of the phases in gas–liquid flows under several flow conditions in vertical and horizontal 67 mm internal diameter pipes. The sampling frequencies for the ECT and WMS were 200 and 1000 Hz, respectively. The test fluids used were air and silicone oil. Data were obtained for a range of superficial velocities that varied from 0.05 to 0.38 m/s for liquid and from 0.05 to 4.72 m/s for gas. The signals from the sensor, that are proportional to the liquid capacitance, are processed to obtain time series of void fraction, frequency and structure velocity. A comparison between the detailed analysis of void fraction distributions in vertical and horizontal pipes for an air–silicone oil mixture has been experimentally investigated. The main conclusions from this study are stated as follows:

1. The flow patterns namely spherical cap bubble, slug and churn flows were observed for the vertical two-phase pipe flow configuration, whilst plug, slug and stratified wavy flows were identified for the horizontal two-phase pipe flow configuration.
2. The results of flow development using the PDF of void fraction obtained at 3 measurement locations; ECT 1, ECT 2 and WMS at 4.4, 4.489 and 4.92 m, respectively, showed that the flow is fully developed and statistically stable for the vertical two-phase flow. While on the other hand, the flow is not fully developed for the horizontal two-phase flow scenario at same liquid and gas superficial velocities.
3. There was a noticeable systematic divergence of measured void fractions between the horizontal and vertical flow configurations at liquid superficial velocities of 0.05 m/s with the horizontal pipe having the higher values. At the highest gas superficial velocity of 4.72 m/s, the vertical and horizontal void fractions are almost identical.
4. The virtual central cut views of the two-phase flow structures obtained by processing of the WMS data show that for vertical pipe flows, the cross-sectional distribution of the void fraction is substantially different to that of the corresponding horizontal pipe configuration passing at the same liquid and gas superficial velocities. The results of the virtual central cut views of the flow structures enables the researcher to gain a better understanding of how liquid and gas phases are distributed during the transition from one flow pattern to another.
5. The computed frequencies of the flow structures were concluded to be larger for the vertical than the horizontal flow configuration when passing the same liquid and gas superficial velocities.
6. A significant difference in flow structure was observed at gas superficial velocity of 4.72 m/s, the vertical two-phase flow structure velocity was seen to be higher than its horizontal counterpart. The observed fluctuations in the values of structure velocity for horizontal two-phase flow can be attributed to the fact that the flow is not fully developed.

7. For the vertical pipe flow configuration, the estimated values of the flux parameter C_0 are 2.52, 1.23 and 1.09 for spherical cap bubble, slug and churn flows, respectively. The estimated values of C_0 concerned with horizontal pipe flow configuration for plug, slug and stratified wavy flows are 2.248, 1.246 and 1.214, respectively. The study confirms the findings of Weber (1981), Nicholson et al. (1978) and Benjamin (1968) that drift velocity exists in horizontal slug flow as a consequence of the balance between lateral and axial pressure gradients.
8. The relationship between horizontal two-phase flow drift velocity and average void fraction is a bell-shaped curve, with the peak value depicting slug flow whilst the two lower ends represent plug and stratified wavy flows.
9. It is concluded that a plot of mixture superficial velocity against average void fraction may be used to provide a qualitative index to determine the flow pattern present, regardless of orientation of the pipe. The magnitude of the computed drift-flux coefficients C_0 and V_D are related significantly to the pipe orientation and flow patterns.

Acknowledgment

Abdulkadir, M., would like to express his sincere appreciation to the Nigerian government through the Petroleum Technology Development Fund (PTDF) for providing the funding for his doctoral studies.

This work has been undertaken within the Joint Project on Transient Multiphase Flows and Flow Assurance. The Author(s) wish to acknowledge the contributions made to this project by the UK Engineering and Physical Sciences Research Council (EPSRC) and the following: - GL Industrial Services; BP Exploration; CD-adapco; Chevron; ConocoPhillips; ENI; ExxonMobil; FEESA; IFP; Institutt for Energiteknikk; PDVSA (INTEVEP); Petrobras; PETRONAS; SPT; Shell; SINTEF; Statoil and TOTAL. The Author(s) wish to express their sincere gratitude for this support.

References

Abdulahi, A., Abdulkareem, L.A., Sharaf, S., Abdulkadir, M., Hernandez Perez, V., Azzopardi, B.J., 2011. Investigating the effect of pipe inclination on two-phase gas–liquid flows using advanced instrumentation. In: Proceedings of the ASME/JSME 8th Thermal Engineering Joint Conference, March 13–17, 2011, Honolulu, Hawaii, USA, AJTEC2011-44239.

Abdulkadir, M., Hernandez-Perez, V., Lowndes, I.S., Azzopardi, B.J., Brantson, E.T., 2014a. Detailed analysis of phase distributions in a vertical riser using wire mesh sensor (WMS). Exp. Therm. Fluid Sci. 59, 32–42.

Abdulkadir, M., Hernandez-Perez, V., Lowndes, I.S., Azzopardi, B.J., Sharaf, S., 2010. Experimental investigation of phase distributions of two-phase air–silicone oil flow in a vertical pipe. World Acad. Sci. Eng. Technol. 4, 18–25.

Abdulkadir, M., Zhao, D., Sharaf, S., Abdulkareem, L.A., Lowndes, I.S., Azzopardi, B.J., 2011. Interrogating the effect of 90° bends on air–silicone oil flows using advanced instrumentation. Chem. Eng. Sci. 66, 2453–2467.

Abdulkadir, M., Hernandez-Perez, V., Lowndes, I.S., Azzopardi, B.J., Dzomeku, S., 2014b. Experimental study of the hydrodynamic behaviour of slug flow in a vertical riser. Chem. Eng. Sci. 106, 60–75.

Abdulkadir, M., Hernandez-Perez, V., Lowndes, I.S., Azzopardi, B.J., 2015. Comparison of experimental and computational fluid dynamics (CFD) studies of slug flow in a vertical riser. Exp. Therm. Fluid Sci. 68, 468–483.

Abdulkadir, M., Hernandez-Perez, V., Lo, S., Lowndes, I.S., Azzopardi, B.J., 2013. Comparison of Experimental and Computational Fluid Dynamics (CFD) studies of slug flow in a vertical 90° bend. J. Comput. Multiphase Flows 5, 265–281.

Abdulkadir, M., Hernandez-Perez, V., Lowndes, I.S., Azzopardi, B.J., Sam-Mbomah, E., 2016. Experimental study of the hydrodynamic behaviour of slug flow in a horizontal pipe. Chem. Eng. Sci. 156, 147–161.

Abdulkareem, L.A., Hernandez Perez, V., Sharaf, S., Azzopardi, B.J., 2011. Characteristics of air–oil slug flow in inclined pipe using tomographic techniques, In: Proceedings of the ASME/JSME 8th Thermal Engineering Joint Conference, March 13–17, 2011, Honolulu, Hawaii, USA, AJTEC2011–44546.

Azzopardi, B.J., Abdulkareem, L.A., Zhao, D., Thiele, S., da Silva., M.J., Beyer, M., Hunt, A., 2010. Comparison between electrical capacitance tomography and wire mesh sensor output for air/silicone oil flow in a vertical pipe. Ind. Eng. Chem. Res. 49.

Barbosa, J.R., Govan, A.H., Hewitt, G.F., 2001. Visualization and modelling studies of churn flow in a vertical pipe. Int. J. Multiph. Flow 27, 2105–2127.

Bendiksen, K.H., 1984. An experimental investigation of the motion of long bubbles in inclined tubes. Int. J. Multiph. Flow 10, 467–483.

Benjamin, T.B., 1968. Gravity current and related phenomena. J. Fluid Mech. 31 (part 2), 224.

Bhagwat, S.M., Ghajar, A.J., 2014. A flow pattern independent drift-flux model based void fraction correlation for a wide range of gas–liquid two-phase flow. Int. J. Multiph. Flow 59, 186–205.

Bonnecaze, K.H., Erskine, W., Greskovich, E.J., 1971. Holdup and pressure drop for two-phase slug flow in inclined pipelines. AIChE J. 17, 1109–1113.

Brown, D.J., Jensen, A., Whalley, P.B., 1975. Non-equilibrium effects in heated and unheated annular two-phase flow. ASME Paper 75, 754–757.

da Silva, M.J., Schleicher, E., Hampel, U., 2007. Capacitance wire-mesh sensor for fast measurement of phase fraction distributions. Measur. Sci. Technol. 18, 2245–2251.

Dinaryanto, O., Prayitno, Y.A.K., Majid, A.I., Hudaya, A.Z., Nusirwan, Y.A., Widyaparaga, A., Indarto, Deendarlianto, 2017. Experimental investigation of the initiation and flow development of gas–liquid slug two-phase flow in a horizontal pipe. Exp. Therm. Fluid Sci. 81, 93–108.

Dukler, A.E., Hubbard, M.G., 1984. A model for gas–liquid slug flow in horizontal and near horizontal tubes. Ind. Eng. Chem. Fundam. 14, 337–347.

Franca, F., Lahey, R.T., 1992. The use of drift-flux techniques for the analysis of horizontal two-phase flows. Int. J. Multiph. Flow 18, 787–801.

Geraci, G., Azzopardi, B.J., Maanen, H.R.E., 2007. Effect of inclination on circumferential film thickness variation in annular gas/liquid flow. Chem. Eng. Sci. 62, 3032–3042.

Gokcal, B., 2006. An experimental and theoretical investigation of slug flow for high oil viscosity in horizontal pipes. University of Tulsa. PhD thesis.

Gomez, L.E., Shoham, O., Schmidt, Z., Chokshi, R.N., Northug, T., 2000. Unified mechanistic model for steady-state two-phase flow: horizontal to vertical upward flow. SPE J. 5, 339–350.

Hazuku, T., Takamasa, T., Matsumoto, Y., 2008. Experimental study on axial development of liquid film in vertical upward annular two-phase flow. Int. J. Multiph. Flow 34, 111–127.

Hernandez-Perez, V., 2008. Gas–liquid two-phase flow in inclined pipes. University of Nottingham. PhD thesis.

Hernandez-Perez, V., Abdulkadir, M., Azzopardi, B.J., da Silva, M.J., 2010. Effects of pipe inclination on the internal structure of the liquid slug body. In: 7th International Conference on Heat Transfer, Fluid Mechanics and Thermodynamics, 19–21 July 2010 Antalya, Turkey.

Hubbard, M.G., Dukler, A.E., 1966. The characterization of flow regimes for horizontal two-phase flow I. Statistical analysis of wall pressure fluctuations. In: Proceedings of Heat Transfer and Fluid Mechanics, Institute Stanford University Press, pp. 385–400.

Julia, J.E., Ozar, B., Dixit, A., Jeong, J.J., Hibiki, T., Ishii, M., 2009. Axial flow development of flow regime in adiabatic upward two-phase flow in a vertical annulus. J. Fluids Eng.-T ASME 131, 0213021–02130211.

Kaji, R., Azzopardi, B.J., Lucas, D., 2009. Investigation of flow development of co-current gas–liquid vertical slug flow. Int. J. Multiph. Flow 35, 335–348.

Kataoka, I., Ishii, M., 1987. Drift-flux model for large diameter pipe and new correlation for pool void fraction. Int. J. Heat Mass Transf. 30, 1927–1939.

Nicholson, K., Aziz, K., Gregory, G.A., 1978. Intermittent two phase flow in horizontal pipes, predictive models. Can. J. Chem. Eng. 56, 653–663.

Nicklin, D.J., Wilkes, J.O., Davidson, J.F., 1962. Two-phase flow in vertical tubes. Trans. Inst. Chem. Eng. 156, 61–68.

Pereyra, E., Torres, C., 2005. FLOPATN—Flow Pattern Prediction and Plotting Computer Code. The University of Tulsa, Tulsa, Oklahoma, USA.

Prasser, H.-M., Bottger, A., Zschau, J., 1998. A new electrode-mesh tomograph for gas–liquid flows. Flow Measur. Instrum. 9, 111–119.

Roitberg, E., Shemer, L., Barnea, D., 2007. Measurements of cross-sectional instantaneous phase distribution in gas–liquid pipe flow. Exp. Therm Fluid Sci. 31, 867–875.

Shoham, O., 2006. Mechanistic Modelling of Gas–Liquid Two-Phase Flow in Pipes. University of Tulsa, Society of Petroleum Engineers, USA.

Szalinski, L., Abdulkareem, L.A., da Silva, M.J., Thiele, S., Beyer, M., Lucas, D. Hernandez, Perez, V., Azzopardi, B.J., Hampel, U., 2010. Comparative study of gas–oil and gas–water two-phase flow in a vertical pipe. Chem. Eng. Sci. 65, 3836–3848.

Wallis, G.B., 1969. One Dimensional Two-Phase Flow. McGraw Hill Book Company, New York, pp. 175–281.

Waltrich, P.J., Falcone, G., Barbosa, J.R., 2013. Axial development of annular, churn and slug flows in a vertical tube. Int. J. Multiph. Flow 57, 38–48.

Wang, K., Bai, B., Cui, J., Ma, W., 2012. A physical model for huge wave movement in gas–liquid churn flow. Chem. Eng. Sci. 79, 19–28.

Weber, M.E., 1981. Drift in intermittent two-phase flow in horizontal pipes. Can. J. Chem. Eng. 59, 398–399.

Wolf, A., Jayanti, S., Hewitt, G.F., 2001. Flow development in vertical annular flow. Chem. Eng. Sci. 56, 3221–3235.

Zuber, N., Findlay, J.A., 1965. Average volumetric concentration in two-phase flow systems. J. Heat Transf. Trans. ASME 87, 453–468.